INFLUENCE OF GEOMETRICAL CORRECTNESS ON STEREOSCOPIC VIEWING DURING REAL-TIME TELEMANIPULATION

Stefan Kimmer and André Schiele

Euorpean Space Agency ESTEC, Telerobotics & Haptics Laboratory, Noordwijk,The Netherlands, Email: {stefan.kimmer,andre.schiele}.schiele@esa.int

Faculty of Mechanical, Maritime and Materials Engineering, Delft University of Technology, Delft, The Netherlands

ABSTRACT

In this paper, the influence of geometric correctness in teleoperated stereo vision is analyzed on task execution performance in simple yet realistic teleoperation tasks. Major factors are determined that contribute to geometric distortions in stereoscopic televiewing systems. In a preliminary user experiment the effects of different visual feedback modes on operator performance are analyzed in joystick-based position teleoperation with a KUKA lightweight robot. Performance of three novice users performing positioning tasks is analyzed w.r.t. time to completion and error rate while exposed to a) geometrically correct, b) geometrically distorted, c) monoscopic and d) direct vision feedback from the robotic workcell. First results indicate that distortion free stereo television has no added value on completion time and error rate. It appears that in real-life teleoperation scenarios sufficient other depth-cues are available to help operators interpreting the remotely viewed scene. Even monoscopic television is not clearly disadvantageous.

Key words: Stereoscopic, Teleoperation, 3D.

1. INTRODUCTION

In robotic teleoperation applications, it appears to be commonly perceived that stereo-vision provides added value when needing to position objects or robotic devices in a remotely perceived environment [13] [8]. Recently, the broad arrival of 3D television and 3D cinema has further increased this perception and has triggered research in how to optimally tune stereo vision systems for good and broad user perception [10]. However, such analyses mostly concentrated on eye-strain and user comfort.

In real-life teleoperation scenarios, however, with camera based real-time stereo vision feedback one could argue that also geometric distortions created by the system are relevant. For instance, depth distortions from the camera, the display system and from wrong positioning of the operator in front of the viewing system could have a significant influence on the ability to correctly interpret distances and dimensions of objects in the remotely viewed scene. According to the knowledge of the authors, no study exists so far, in which the influence of geometric correctness in stereo vision feedback systems has been assessed with respect to user perception and performance in real-life teleoperation.

Figure 1. The operator during a teleoperation television experiment looking at the monoscopic view of the workcell with the lightweight robot. The robot is operated with a joystick and the task was to press a small button (in the center of the screen, in front of the robot's tip) from randomized starting positions of the robot manipulator.

If geometric distortions can influence operator performance, the conception of a geometrically correct - as compared to natural human vision - television system would be clearly beneficial for telemanipulation. However, such systems will likely involve higher costs. Therefore, during the preparations for our space-based teleoperation experiment ME-

TERON [15] we decided to perform an analysis and to conceive an experiment to understand the factors involved with geometric correctness in stereo vision. Moreover, we hypothesized that a geometrically correct stereo television system would allow non-trained operators to perform with natural skill without requiring training.

The review provided in [13] states that stereoscopic viewing can improve the task execution performance of real-time dexterous teleoperation. This includes the reduction of task execution time, the improvement of accuracy and the reduction of error rates. In that review, 23 out of 27 experiments from different research institutes have been reviewed and it has been concluded that the usage of a stereoscopic system in spatial manipulation of objects is beneficial. However, none[1] of the experiments explicitly targeted the impact of geometric distortions on the operator performance in the manipulation of objects. Moreover, ten of the experiments were carried out with virtual environments. Real teleoperation environments have been studied in [2][4, Exp.2 & Exp.3][5][7][11][14][16][17][18][19] and [20]. All, except [4, Exp.2] (which has reported mixed benefit) have reported that stereoscopic vision is beneficial for user performance. In [9] the authors mentioned difficulties of keeping the geometries correct in stereo television systems, but the authors did not examine the impacts of those on operators during an experimental campaign.

It is the goal of this paper to analyze the influence of geometric correctness in stereo vision on the task execution performance of human operators in a simple, but realistic teleoperation task. First, this paper will explain which factors can contribute to geometric distortions in stereoscopic viewing - when compared to the human eye. Next, guidelines will be provided for the selection of components to construct geometrically correct "*human centric*" stereo television systems. A preliminary user experiment is presented, analyzing the effects of varying geometrical stereo vision feedback on operator performance in teleoperation with a lightweight robot, involving repetitive positioning tasks. Performance of three novice users is analyzed w.r.t. time to completion and error rate when subjected to a) geometrically correct, b) geometrically distorted, c) monoscopic and d) direct vision onto the same robotic workcell.

2. GEOMETRY OF BINOCULAR TELEVISION

The eye can be modeled as a thick lens where all central rays of light are passing through a nodal point. In general, the rays from a point in space which are

[1]The text of the papers "Cole & Parker 1989" , "Drasnic (1) 1991" and Kama & DuMars 1964 could not be retrieved and hence could not be examined

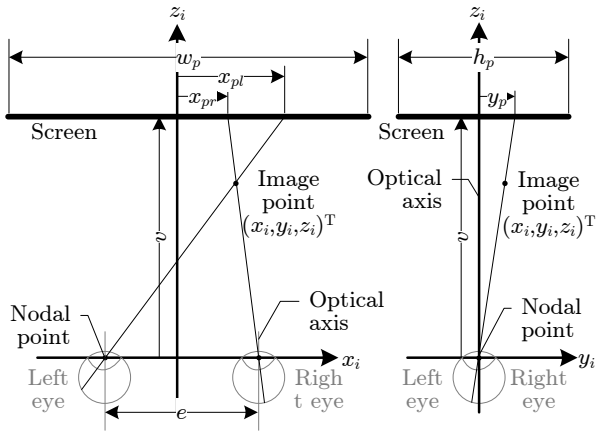

Figure 2. The image space in front of the eyes with a screen capable of displaying a separate image for each eye. Top view on horizontal plane (left) and side view on horizontal plane illustrated (right)

passing through the nodal points of the eyes are hitting the retina at different distances from the optical axis. From this disparity, the human visual system can detect the depth of that point. On a stereoscopic display this point can be displayed on the screen at two different locations in one horizontal line. The symbols x_{pl} and x_{pr} are describing that location for the left and the right eye respectively. If each location is visible to only one eye, the point must be at the intersection of the rays through the nodal points and the points on the screen (see Figure 2). The connecting line segment of the two eyes is assumed to be parallel to the screen. Moreover, the center of that line segment is assumed to be at the center of the screen. With the viewing distance v the image point position is given by

$$\begin{pmatrix} x_i \\ y_i \\ z_i \end{pmatrix} = \frac{1}{e + x_{pl} - x_{pr}} \begin{pmatrix} e(x_{pl} + x_{pr})/2 \\ ey_p \\ ve \end{pmatrix}. \quad (1)$$

A pair of cameras with an equal focal length f and sensor width w_c can be aligned such that the optical axes are parallel to each other. The sensors are shifted by the sensor offset h away from the optical axis. A point of an object is projected on the sensors with the distances of x_{cl} and x_{cr} from the center line in horizontal direction (see Figure 3). In the vertical direction, the point is projected to y_c on both sensors. The term sensor is used here as a synonym for a virtual image plane. That projections of an object point are given by

$$\begin{pmatrix} x_{cl} \\ x_{cr} \\ y_c \end{pmatrix} = \frac{1}{z_o} \begin{pmatrix} f(x_o + b/2) - hz_o \\ f(x_o - b/2) + hz_o \\ fy_o \end{pmatrix}. \quad (2)$$

The whole sensor is displayed on a screen with the magnification factor $m = \frac{w_p}{w_c}$. The magnification is assumed to be constant and homogeneous. This

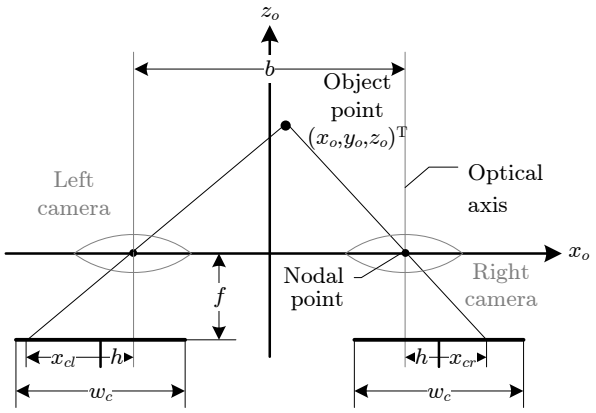

Figure 3. The object space with a pair of cameras. The object point is projected on the two sensors (the thick lines on the bottom). The two sensors are shifted by h away from the optical axes.

results in:

$$\begin{pmatrix} x_{pl} \\ x_{pr} \\ y_p \end{pmatrix} = m \begin{pmatrix} x_{cl} \\ x_{cr} \\ y_c \end{pmatrix} \tag{3}$$

Finally, the whole transformation is expressed by the following formula:

$$\begin{pmatrix} x_i \\ y_i \\ z_i \end{pmatrix} = \frac{1}{mbf + (e - 2hm)z_o} \begin{bmatrix} mef & 0 & 0 \\ 0 & mef & 0 \\ 0 & 0 & ve \end{bmatrix} \begin{pmatrix} x_o \\ y_o \\ z_o \end{pmatrix} \tag{4}$$

This formula corresponds to the one derived in [21] with a camera convergence angle of 0°. The formation of a three-dimensional image of a sample object is illustrated in Figure 4.

To obviate distortions in depth, the summand of the denominator of (4) which is depended on z_o, must be zero. Furthermore, the scaling in all three dimensions must be equal. This results in the following two constraints:

$$h = \frac{e}{2m} \tag{5}$$

$$v = mf \tag{6}$$

If no distortions occur, the three-dimensional image is referred to be ortho-stereoscopic. To get an identical sized image of the object the distance of the eyes and the distance of the cameras must be equal.

$$e = b \tag{7}$$

If this is the case, the image is referred to be tauto-stereoscopic. As a consequence of the model in (4) the stereo camera must be calibrated such that no lens distortions occur, the optical axes of the cameras are parallel, the focal length is the same in both

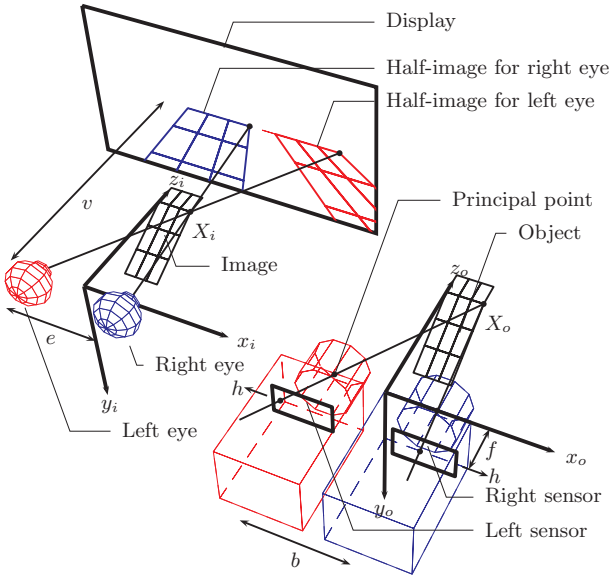

Figure 4. Illustration of the capturing of a point X_o with a stereo camera and the appearance of the corresponding image point X_i in front of a stereoscopic display viewed with two eyes. Several other points are exemplary shown, which together form an object (A planar grid with one bend in z-direction).

cameras, the sensors are on a plane and are not rotated to each other. The operator must be centered to the display.

The constraint of (6) implies that the viewing distance must be changed when the camera zooms the object in or out. If for example the focal length doubles and the operator remains at the previous viewing distance the depth of the image would be scaled to half of the object. In other words, the image appears flatter when zoomed in and more stretched when zoomed out. This effect is illustrated in Figure 5 with a double sized viewing distance and the same object. To examine whether this flattening or stretching impacts the operator's task execution performance, the preliminary experimental campaign shown in Section 3 were performed.

3. USER EXPERIMENTS

It is the goal of this experimental campaign to have a first glimpse on the influence of the geometric correctness in teleoperated stereo vision on user performance. The chosen task is a repetitive randomized positioning task. In this pilot experiment, a small group of three users were tested. The results help to understand first major effects and will be used for the design of a refined and more extensive real experiment.

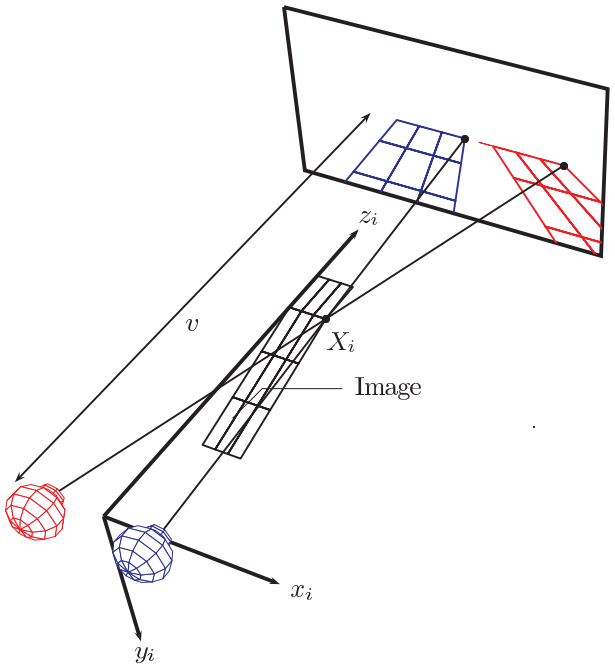

Figure 5. Distorted image with the same parameters as in Figure 4 except a double viewing distance v. The image is stretched twice in the z-dimension

3.1. Experimental Setup

The system used for the experiment consists of a robot attached to a mechanical task-board, a joystick controller and a vision system.

3.1.1. Lightweight Robot Workcell

The robot is a KUKA lightweight robot (LWR) attached to a custom-built experimental task-board that is used for generic telemanipulation analysis. The task-board contains mechanical elements, such as sliders, torque wrenches, peg-in-hole systems, doors and a push button. The KUKA lightweight robot is equipped with a synthetic conic tip that is attached as a tool. This tip can be used to explore the various features of the task-board. The lightweight robot is controlled through a USB 3DOF joystick (Logitech Force 3D Pro) via an external computer that communicates with the KUKA robot controller (KRC) through the robot sensor interface (RSI). The RSI interface in our implementation supports direct joint-space and Cartesian-space control of the manipulator at 4 ms intervals in position and impedance control modes. The robot control software is configured such, that direct telemanipulation commands can be exchanged with autonomous motion commands, for which target Cartesian set-points can be sent to the KRC also through the network interface. For autonomous motion, the KRC internal path-planner is used. Thereby, the implementation of the interface allows smooth transitioning between teleoperated and autonomous movements. The internal forces of the lightweight robot, as well as the estimated forces and torques at the end-effector are provided to the external system for analysis purpose. For the experiment, the control system is configured to move the robot manipulator to random generated Cartesian starting positions that are transmitted from the external PC when a specific button on the joystick is pressed. After the starting position has been reached in Cartesian position control mode, the controller switches to impedance control mode and waits for direct telemanipulation commands transmitted from the joystick axes. The operator can then command the robot manipulator in three Cartesian axes. The three axes are the orthogonal axes of the tool which are orientationally fixed and aligned with the task-board outer borders. Thus, the displacement of the robot takes place with respect to the inclined front surface of the task-board (see Figure 6). Triggering a specified joystick button causes the robot to re-treat along a straight line that passes through the tool center by −10 cm (used during the experiment to clear from the task-board surface after contact) and then advance in Cartesian position control mode to the new, random generated, starting position transmitted from the experiment PC.

The task-board has a plane surface with several knobs located up to 20 cm above the surface. In addition, there are multiple holes which are aligned in a rectangular pattern. There are also two drawers with lines parallel to the outer edge of the task-board. This allows for regular patterns monoscopic depth cues [12, p. 163]. The task-board is illuminated with several fluorescent tubes from approximately 5 m above. This allows for monoscopic depth cues from shading and cast shadows. The conic tip of the manipulator casts a slight shadow onto the task-board. The task-board is equipped with a push-button which illuminates a light while pressed (Figure 6).

Integrated with the task-board is a smartphone that runs an application displaying a large colored screen area. The display is green when the forces between the robot and the task-board are below a threshold, which is set to 8 N. If the robot presses stronger on the surface, the display changes from green to red. The mobile phone runs an Android application that receives values directly from the experiment PC connected with the KRC controller.

An external camera is used to record the experiments. This video recording is used for post-processing of the experiment. It can be clearly seen in the video, when the button is pressed and what the status of the force indicator is on the mobile phone. An overview of the setup is shown in Figure 6

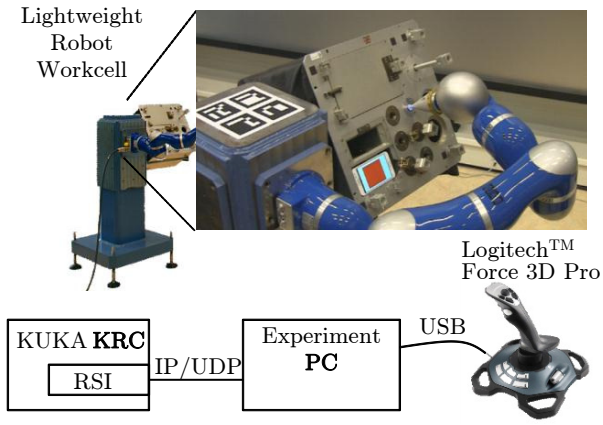

Figure 6. Overview of the setup. The image on the top right is a sample monoscopic view during an experiment. The KUKA robotic arm is pressing the button which consequently is illuminated. The smartphone is red colored which indicates that the force is exceeding a threshold.

3.1.2. Vision System

The vision system consists of a stereo-camera, a display and a processing computer. The stereo-camera consists of two Allied Vision Technology Prosilica GX2300c cameras. Both cameras are equipped with a Kodak KAI-04050 sensor with a maximum resolution of 2336px horizontal and 1752px vertical. A low radial distortion lens LM8HC from KOWA is mounted on the cameras. The images are transferred to a computer which packs the left and right line by line such that only every second line from the respective image is used. This combined image is transferred to the stereoscopic display. The cameras are adjusted such that the optical lines are parallel and passing through the center of the active sensor region. Using adjustment screws the left and the right image can be adjusted such that no vertical parallax emerges (y_p is equal for both images). For monoscopic vision only the left image is fed to the display. The view of that monoscopic image can be seen in Figure 6.

The stereoscopic display is a JVC GD-463D10E liquid crystal display monitor. The operator is wearing circular polarized glasses to ensure that the odd lines from the stereoscopic display are visible only by the left eye and the even lines only by the right eye. The size of the display is 1024 mm with 1920px horizontally and 576 mm with 1080px vertically. Since the separation of the left and right half image is done by alternating polarization of each row the effective resolution in the vertical dimension is half of the total resolution. While the operator is seated in front of the stereoscopic display, a direct view on the real lightweight robot workcell is blocked by a curtain. The parameters used for the experiment are listed in Table 1. The sensor size w_c is expressed in pixels since the focal length f can be measured more accurately in pixels. The focal length is measured using the calibration tool from the OpenCV library ([1]).

Table 1. Values of the parameters for the experiment

Symbol	Value	Designation
f	1508 px	focal length
b	63 mm	camera distance
h	59 px	sensor offset
w_c	1920 px	sensor width
w_p	1024 mm	screen width
m	1024 mm/1920 px	screen magnification
v	80 cm	viewing distance
v	160 cm	viewing distance (distorted)

3.2. Experiment Method

To assess the performance of non-trained subjects, three novice test subjects have been selected. Each subject has been briefly trained how to use the joystick interface with a direct view on the robot. For this training session, which lasted 1 to 5 minutes, the viewing angle was chosen different than for the actual experiment.

For the real experiment set, the subjects have been instructed to use the joystick to "*press the push-button on the task-board with the LWR without causing other contacts with the task-board*". It was the scope to move the tip of the conic end-effector of the robot to the push button and then press it down in a stiff impedance control mode. The robot end-effector is programmed to drive in a plane parallel to the surface of the task-board by the joystick. The subjects were told that the task-board and the robot tip are sensitive and can be broken when contacting to hard. By moving the joystick (left/right and up/down) and the "fire" button of the joystick (forward/backward) the robot can be directly moved left/right, up/down and forward/backward respectively. While pressing the push-button on the task-board with the robot, the button lights up, which indicated to the subjects that they can advance to the next trial. Each trial had a different random starting position of the robot in front of the task-board. To indicate the start for the next trial, the button light was toggled on remotely by the experimenter. Subjects were instructed to start motion, when the light went off.

For each visual condition, 8 trials are executed by each subject, thus a total of 32 trials per subject. The sequence of visual conditions presented to the subjects have not been randomized, since it is assumed that no training effects occur within each trial. Following sequence of visual conditions has been tested:

(1) *Geometrically correct stereoscopic view*, "3D", in which the subject was located 80 cm in front of the center of the 3D screen. The pose of the head of the subjects was constrained by the glasses, which were mounted to a tripod with a fixed location (see Figure 1).

(2) *Geometrically distorted stereoscopic view*, "Distorted 3D", in which the subject was located 160 cm in front of the center of the 3D screen, causing significant depth distortion effects. Thereby the z_i-dimension is twice the z_o-dimension (see Figure 5). Again, the pose of the head was constrained by fixed glasses on a tripod.

(3) *Monoscopic view*, "2D", in which the subject looked at a monoscopic view through glasses, again constrained at the center of the screen at a distance of 80 cm.

(4) *Direct view*, "Direct", in which the subject was standing on the exact same location where otherwise the stereo camera system was located. For this condition, the subject was instructed to not excessively use the neck and torso while executing the experiment.

During all trials, the subjects had been informed that if the smartphone screen shows red color, this would be counted as an error since the interface force between the robot manipulator and the task-board is high. After the experiments, the video recording was used to determine the time to completion for each trial and the number of errors.

3.3. Metrics and Analysis

The independent variable of the experiment is the viewing method. These are the four visual conditions described in Section 3.2. The dependent variables are the time to completion for each trial and the error rate. An error is considered a contact of the robot with the task-board if the threshold of the forces is exceeded (3.1.1). The influence of the independent variables on the dependent ones was checked by statistical analysis (paired t-testing and analysis of variance (ANOVA) with multiple comparison tests.)

4. RESULTS

In Figure 7 boxplots are shown for all experiment trials of the subject group over the four viewing conditions. The ANOVA has shown that the time to completion is less for the "Direct" viewing than for the "3D" view ($p = 0.004$) and the "2D" view ($p = 0.004$). However, the "Direct" viewing method is indifferent from the "Distorted 3D" viewing method.

Figure 8 shows the times to completion for each

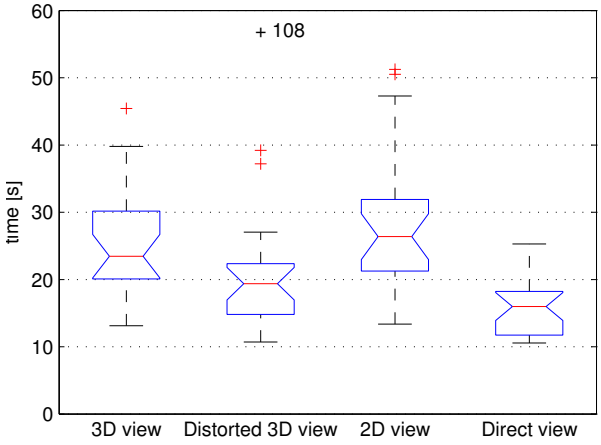

Figure 7. Boxplots of all four viewing methods for the subject group. An outlier is indicated under the "Distorted 3D" view condition, which took 108 s *to complete one trial.*

subject over each trial and viewing condition. The time to completion is most constant in the "Direct" viewing condition, whereas in the other three viewing methods, more variance in the completion times can be seen. However, the graphs show no clear trend that could indicate a significant learning effect over each test round. Subject 3 has the largest variation in execution times.

The total numbers of errors per viewing condition

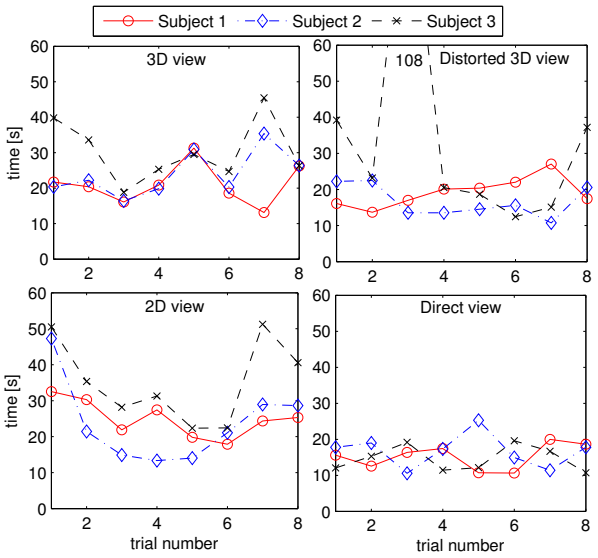

Figure 8. Measurements of the task execution times for all three subjects and all four viewing methods for each experiment trial. At the distorted 3D view the value of Subject 3 and trial number 3 is at 108 s*, which is the outlier depicted in Figure 7.*

and per individual subject is summarized in Figure 9. Subject 3 is the largest contributor to the overall errors. The largest number of all errors is 10 per 8 tri-

als in the "Distorted 3D" view condition and in the "2D view" condition. However, in the "Distorted 3D view" condition, the contribution of error is exclusively from Subject 3. The least total error is in the "Direct view" condition.

5. DISCUSSION

The time to completion with geometrically correct stereoscopic view was not better than with geometrically distorted stereoscopic view. In contrast, the distribution of data could indicate an even better performance under geometrically distorted view. This could perhaps be attributed to the enlarged depth scaling in the image. But also, other factors than geometric distortion can be relevant for the time to completion. Subject 3 reported that it was problematic to focus the screen during the "Distorted 3D" view, due to the large distance from the screen. The many errors of subject 3 can be associated with that. Excluding the results of the error of subject 3 the "Distorted 3D" has performed the best with respect to error rate. This indicates that also for this metric, other factors rather than distortion in depth can be the cause. Those factors may evolve from the discrete nature of the display. The close viewing distance of only 80 cm from the screen causes each pixel to be perceived individually. This effect is intensified by the fact that only every second line is visible for the respective eye due to the polarization. This line separation was reported by all subjects to be "unpleasant". In the "Distorted 3D" case the viewing distance was 160 cm which caused the resolution of the display to subjectively exceed the resolution of the eye.

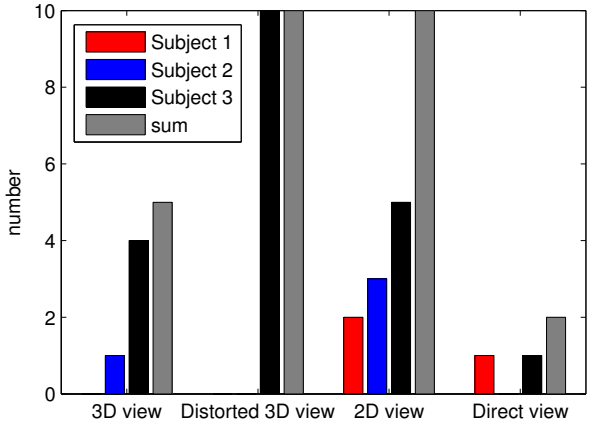

Figure 9. Number of errors made by the subjects during each viewing method. An error was a too hard contact between the robot and the task-board when the press-button was not pressed. The rightmost bar in each series signifies the cumulated sum of errors of all three subjects.

With respect to learning, there could be an indication of a learning effect between the trials that took place in "3D view" and in "Distorted 3D view". When looked at the plots in Figure 8 without the contributions of Subject 3, one could argue that the plots are less scattered for the "3D Distorted" condition then for "3D view". This could explain why a trend towards less time to completion for the distorted condition can be seen also in the boxplots and could explain the fewer errors. In the "2D" view a learning curve may also exist. This is reasonable since the user must learn how to use monoscopic cues while relying on the binocular cues at the previous run. [6] has studied this effect. This indicates strongly that for the full experiment, also the visual conditions need randomization.

All subjects reported that they deliberately chose to make use of shadows in the monoscopic view to estimate the position of tip of the robot with respect to the task-board.

The camera calibration tool (see Section 3.1.2) found a radial lens distortion which is introducing an absolute maximal horizontal difference at the outer corners of the display of $\approx$ 21 px. This introduces a much smaller distortion of the three-dimensional image with respect to the distortion intentionally introduced by doubling the viewing distance. Furthermore, the interpupillary distance (distance of the eyes e) of the operator has a linear influence on the overall scale of the three-dimensional image ((4) with (5) & (6)). In other words, if $e = ab$ then the image is scaled by the factor a in all three dimensions. If a male operator is at the 95th percentile ($e = 71$ mm [3]) the image is scaled by a factor of ≈ 1.13. This is again a much smaller distortion than the one introduced by the doubling of the viewing distance (a factor of 2).

6. CONCLUSIONS AND FUTURE WORK

Direct vision on the task-board allows best performance with respect to time to completion for manipulative teleoperation tasks. Surprisingly, the three television conditions did not significantly differ in performance with respect to time to completion for these experiments. Monoscopic viewing has greatly benefited from shadows that have been used by the test persons as depth cues. To truly verify the influence of geometrical distortions of a three-dimensional image, other factors such as the display resolution must be better controlled. The change of the focal length or the screen magnification always affects the visible details of the object. This effect most likely influences the performance. More subjects must be used in a more extensive campaign to better compensate for variability in the human factors. Further a proper subjective load questionnaire must be made

to be able to account for e.g. mental load differences between the viewing methods. For excluding coupled learning effects between viewing conditions, they must be randomized.

REFERENCES

1. G. Bradski and A. Kaehler. *Learning OpenCV: Computer Vision with the OpenCV Library*. Software that sees. O'Reilly Media, Incorporated, 2008.

2. R. E. Cole and D. L. Parker. Stereo TV improves manipulator performance. In *Proc. SPIE, Three-Dimensional Visualization and Display Technologies*, volume 1083, pages 18–27, 1989.

3. N. A. Dodgson. Variation and extrema of human interpupillary distance. In *Proc. SPIE 5291*, pages 36–46, 2004.

4. J. Draper, S. Handel, C. Hood, and C. Kring. Three experiments with stereoscopic television: When it works and why. In *Systems, Man and Cybernetics, 1991. Decision Aiding for Complex Systems, Conference Proceedings., 1991 IEEE International Conference on*, pages 1047 –1052 vol.2, oct 1991.

5. D. Drascic and J. J. Grodski. Using stereoscopic video for defense teleoperation. In *Proc. SPIE, Stereoscopic Displays and Applications*, volume 1915, pages 58–69, sep 1993.

6. D. Drascic, P. Milgram, and J. Grodski. Learning effects in telemanipulation with monoscopic versus stereoscopic remote viewing. In *Systems, Man and Cybernetics, 1989. Conference Proceedings., IEEE International Conference on*, pages 1244 –1249 vol.3, nov 1989.

7. A. A. Dumbreck, E. Abel, and S. Murphy. 3-D TV system for remote handling: Development and evaluation. In J. O. Merritt and S. S. Fisher, editors, *Proc. SPIE, Stereoscopic Displays and Applications*, volume 1256, pages 226–236, 1990.

8. M. Ferre, R. Aracil, and M. A. S??nchez-Ur??n. Stereoscopic human interfaces. *Robotics Automation Magazine, IEEE*, 15(4):50 –57, dec. 2008.

9. W.-k. Fung, W.-t. Lo, Y.-h. Liu, and N. Xi. A case study of 3D stereoscopic vs. 2D monoscopic tele-reality in real-time dexterous teleoperation. In *Intelligent Robots and Systems, 2005. (IROS 2005). 2005 IEEE/RSJ International Conference on*, pages 181 – 186, aug. 2005.

10. M. Lambooij, W. IJsselsteijn, M. Fortuin, and I. Heynderickx. Visual discomfort and visual fatigue of stereoscopic displays: A review. *Journal of Imaging Science and Technology*, 53(3):030201???030201–14, 2009.

11. B. C. Lee and M. E. Katafiaz. Evaluation of a 3D autostereoscopic display for telerobotic operations. In *Proc. SPIE, Stereoscopic Displays and Virtual Reality Systems*, pages 48–58, 1997.

12. H. A. Mallot and J. S. Allen. *Computational Vision: Information Processing in Perception and Visual Behavior*. Computational Neuroscience. MIT Press, 2000.

13. J. P. McIntire, P. R. Havig, and E. E. Geiselman. What is 3D good for? a review of human performance on stereoscopic 3D displays. In *Proc. SPIE, Head- and Helmet-Mounted Displays XVII; and Display Technologies and Applications for Defense, Security, and Avionics VI*, volume 8383, pages 83830X–1 – 83830X–13, 2012.

14. J. O. Merritt, R. E. Cole, and C. Ikehara. A rapid-sequential-positioning task for evaluating motion parallax and stereoscopic 3D cues in teleoperator displays. In *Systems, Man and Cybernetics, 1991. Decision Aiding for Complex Systems, Conference Proceedings., 1991 IEEE International Conference on*, pages 1041 –1046 vol.2, oct 1991.

15. A. Schiele. METERON - validating orbit-to-ground telerobotics operations technologies. In *11th Symposium on Advanced Space Technologies in Robotics and Automation, ASTRA 2011*, 2011.

16. D. R. Scribner and J. W. Gombash. The effect of stereoscopic and wide field of view conditions on teleoperator performance. Final rept., Army Research Lab Aberdeen Proving Ground Md Human Research And Engineeringdirectorate, mar 1998.

17. D. C. Smith, R. E. Cole, J. O. Merritt, and R. L. Pepper. Remote operator performance comparing mono and stereo tv displays: the effects of visibility, learning and task factors. Technical Report 380, Naval Ocean Systems Center, San Diego, California, 1979.

18. D. C. Smith and R. L. Pepper. Stereo TV improves operator performance under degraded visibility conditions. *Optical Engineering*, 20:74–83, aug 1980.

19. E. H. Spain. Stereo advantage for a peg-in-hole task using a force-feedback manipulator. In *Proc. SPIE, Stereoscopic Displays and Applications*, volume 1256, pages 244–254, 1990.

20. E. H. Spain and K.-P. Holzhausen. Stereoscopic versus orthogonal view displays for performance of a remote manipulation task. In *Proc. SPIE 1457, Stereoscopic Displays and Applications II*, volume 1457, pages 103–110, aug. 1991.

21. A. Woods, T. Docherty, and R. Koch. Image distortions in stereoscopic video systems. In *Proceedings of the SPIE Volume 1915, Stereoscopic Displays and Applications IV*, 1993.